J Physiol 590.13 (2012) pp 3185–3202

The Journal of Physiology

The chemokine CXCL12 and the HIV-1 envelope protein gp120 regulate spontaneous activity of Cajal–Retzius cells in opposite directions

Ivan Marchionni, Michael Beaumont and Gianmaria Maccaferri

Department of Physiology, Feinberg School of Medicine, Northwestern University, Chicago, IL 60611, USA

Key points

- The CXC chemokine ligand 12 (CXCL12) modulates spontaneous firing of Cajal–Retzius cells via the CXC chemokine receptor 4 (CXCR4). However, the underlying mechanism(s) are poorly understood. CXCR4 also binds the human immunodeficiency virus type 1 (HIV-1) envelope glycoprotein 120 (gp120), but the functional effects of this interaction on Cajal–Retzius cell excitability remain unknown.
- We show that CXCL12 reduces spontaneous firing in Cajal–Retzius cells by opening a BK-type calcium-activated potassium conductance, whereas gp120 increases their excitability via a calcium- and chloride-dependent mechanism.
- Our data suggest that, depending on the use of CXCL12 or gp120 as ligands, partial agonism at the CXCR4 receptor generates calcium responses of different strengths, which lead to the recruitment of either calcium-activated potassium or chloride channels.
- We propose that HIV infection disrupts a signalling pathway important for the regulation of the excitability of Cajal–Retzius cells, and alters their functions.

Abstract Activation of the CXC chemokine receptor 4 (CXCR4) in Cajal–Retzius cells by CXC chemokine ligand 12 (CXCL12) is important for controlling their excitability. CXCR4 is also a co-receptor for the glycoprotein 120 (gp120) of the envelope of the human immunodeficiency virus type 1 (HIV-1), and binding of gp120 to CXCR4 may produce pathological effects. In order to study CXCR4-dependent modulation of membrane excitability, we recorded in cell-attached configuration spontaneous action currents from hippocampal stratum lacunosum-moleculare Cajal–Retzius cells of the CXCR4-EGFP mouse. CXCL12 (50 nM) powerfully inhibited firing independently of synaptic transmission, suggesting that CXCR4 regulates an intrinsic conductance. This effect was prevented by conditioning slices with BAPTA-AM (200 μM), and by blockers of the BK calcium-dependent potassium channels (TEA (1 mM), paxilline (10 μM) and iberiotoxin (100 nM)). In contrast, exposure to gp120 (pico- to nanomolar range, alone or in combination with soluble cluster of differentiation 4 (CD4)), enhanced spontaneous firing frequency. This effect was prevented by the CXCR4 antagonist AMD3100 (1 μM) and was absent in EGFP-negative stratum lacunosum-moleculare interneurons. Increased excitability was prevented by treating slices with BAPTA-AM or bumetanide, suggesting that gp120 activates a mechanism that is both calcium- and chloride-dependent. In conclusion, our results demonstrate that CXCL12 and gp120 modulate the excitability of Cajal–Retzius cells in opposite directions. We propose that CXCL12 and gp120 either generate calcium responses of different strength or activate distinct pools of intracellular calcium, leading to agonist-specific

DOI: 10.1113/jphysiol.2011.224873

responses, mediated by BK channels in the case of CXCL12, and by a chloride-dependent mechanism in the case of gp120.

(Received 18 November 2011; accepted after revision 1 April 2012; first published online 2 April 2012)
Corresponding author G. Maccaferri: Northwestern University, Dept of Physiology, Feinberg School of Medicine, 303 E Chicago Ave, Tarry Blg Rm 5-707, Chicago, IL 60611, USA. Email: g-maccaferri@northwestern.edu

Abbreviations ACSF, artificial cerebrospinal fluid; CD4, cluster of differentiation 4; CXCL12, chemokine (C-X-C motif) ligand 12; CXCR4, CXC chemokine receptor 4; CXCR7, CXC chemokine receptor 7; EGFP, enhanced green fluorescent protein; gp120, glycoprotein 120; HIV-1, human immunodeficiency virus type 1; KCC2, K^+–Cl^- cotransporter 2; RT, room temperature; SDF-1α, stromal cell-derived factor-1α.

Introduction

Cajal–Retzius cells are special pioneer neurons of the marginal zone, believed to play important roles for the development and regulation of cortical circuits (for reviews see: Frotscher, 1998; Mienville, 1999; Soriano & Del Río, 2005). In the hippocampus, they are involved in guiding the correct layer-specific positioning of entorhinal inputs (Del Río *et al.* 1997; Borrell *et al.* 1999) and control granule cell migration by acting on the radial glia scaffold (Frotscher *et al.* 2003). These functions are mediated by the glycoprotein reelin, of which Cajal–Retzius cells are a critical cellular source (Ogawa *et al.* 1995). At later developmental stages, Cajal–Retzius cells have been suggested to act as local-circuit neurons, regulating the integrative functions of hippocampal stratum lacunosum-moleculare (Marchionni *et al.* 2010; Maccaferri, 2011) and neocortical layer I (Radnikow *et al.* 2002).

Direct recordings from these cells in the postnatal neocortex and hippocampus have revealed the presence of spontaneous firing (Mienville, 1998, Marchionni *et al.* 2010), suggesting that this tonic activity may be important for their regulation of local circuit processing (Marchionni *et al.* 2010; Maccaferri, 2011).

How is the intrinsic firing of Cajal–Retzius cells modulated? Different studies, again, both in the neocortex and hippocampus, have shown that GABAergic signalling to Cajal–Retzius cells appears to remain excitatory and does not undergo the excitatory/inhibitory shift observed in other neurons (Mienville, 1998; Marchionni *et al.* 2010). The explanation underlying this observation is that Cajal–Retzius cells express the NKCC1 (Achilles *et al.* 2007), but not the KCC2 transporter (Pozas *et al.* 2008). Hence, they maintain high concentrations of intracellular chloride that make $GABA_A$ receptor-mediated input excitatory. Therefore, conventional GABAergic synaptic inhibition is unlikely to be involved.

Recent work in the postnatal hippocampus has shown that CXCL12 (also referred to as stromal cell-derived factor 1α, SDF-1 α, see Guyon & Nahon, 2007 for a review on its effects on the brain) can abolish spontaneous firing in these neurons by hyperpolarizing their membrane potential to subthreshold values (Marchionni *et al.* 2010). This effect is mediated by the activation of the CXC chemokine receptor 4 (CXCR4), which is expressed by Cajal–Retzius cells (Stumm *et al.* 2002, 2003). However, the detailed sequence of events leading from receptor activation to membrane hyperpolarization (including the conductance mediating this effect) remains unknown.

Here, we have directly investigated the molecular events triggered by CXCR4 activation that lead to the suppression of their spontaneous activity. Our results show that reduced excitability is critically mediated by an increase in intracellular calcium levels and by the activation of a BK-type calcium-dependent potassium conductance.

In addition, CXCR4 is also a co-receptor for the HIV-1 virus (Feng *et al.* 1996), and binding of the HIV-1 envelope glycoprotein gp120 to CXCR4 can trigger functional effects in neurons (Davis *et al.* 1997; Meucci *et al.* 1998). For these reasons, we have also investigated whether gp120 affects Cajal–Retzius cell excitability in a manner similar to CXCL12. Surprisingly, our results demonstrate that CXCL12 and gp120 produce opposite results, and thus suggest that the disruption of electrical activity of Cajal–Retzius cells may underlie part of the pathophysiology of cortical circuits in fetal/infant HIV-1 infections.

Methods

Ethical approval

All experimental procedures described in the present work were in accordance with the National Institute of Health (NIH) guidelines for the Care and Use of Laboratory Animals and following Northwestern University Institutional Animal Care and Use Committee (IACUC) approved protocols. We have read *The Journal of Physiology* policy and UK Regulations on Animal Experimentation (Drummond, 2009), and our experiments complied with the policies and regulations.

Slice preparation

Hippocampal slices were prepared from a total of $n = 91$ P14–P20 CXCR4-EGFP mice (www.gensat.org) in order

to be able to target Cajal–Retzius cells, which, at this developmental stage, are the only cellular population of stratum lacunosum-moleculare expressing EGFP (Marchionni *et al.* 2010). Mice were deeply anaesthetized using isoflurane. Following deep anaesthesia, mice were quickly decapitated and the brain put in a small container filled with chilled 'cutting' artificial cerebrospinal fluid (ACSF) of the following composition (in mM): 130 NaCl, 24 $NaHCO_3$, 3.5 KCl, 1.25 NaH_2PO_4, 1 $CaCl_2$, 2 $MgCl_2$, 10 glucose saturated with 95% O_2–5% CO_2 at pH 7.4. A vibratome (Leica, VT 1200 S) was used to cut sections of 350 μm in the same solution. Slices were stored in 'recording' ACSF with modified $CaCl_2$ and $MgSO_4$ concentrations (2 mM and 1 mM, respectively), held at 30°C for the initial 30 min, and at room temperature (RT) afterwards until use. In the experiments of Fig. 6*C*, 1 μM AMD3100 was present during the recovery period. In the experiments of Fig. 6*D*, extracellular KCl was raised to 7–10 mM in order to trigger spontaneous firing in interneurons.

BAPTA-AM-conditioned slices

The experiments of Figs 4*A* and 9 were performed on slices incubated in recording solution containing BAPTA-AM (200 μM) for 1 h. BAPTA-AM was then washed out, and recordings were performed within 45 min from BAPTA-AM removal (Andrade & Rossi, 2010).

Electrophysiological methods

Slices were superfused with pre-heated 'recording' ACSF maintained at a constant temperature (29.5–30.5°C). Fluorescence of EGFP-containing cells was excited by a X-Cite Series 120 light source (Exfo, Ontario, Canada) and visualized using a VE1000 camera (DAGE-MTI, Michigan City, IN, USA). Cells were selected for recording by means of a 60× IR immersion DIC objective applied to a direct microscope (Olympus, Japan). Conventional whole-cell and cell-attached patch-clamp recordings were performed. Pipettes were pulled from borosilicate thin glass capillaries and filled with filtered solution to a final resistance of ∼3 MΩ. Recordings were carried out using a Multiclamp 700B amplifier (Molecular Devices, Sunnyvale, CA, USA). Data were filtered at 3 kHz and digitized at 10–20 kHz using a Digidata A/D board and the Clampex 9 program suite (Molecular Devices). For whole-cell experiments, series and membrane input resistance were monitored by injecting a −5 pA pulse in current-clamp configuration. Series resistances were balanced via a bridge circuit in current-clamp mode. Drugs were bath applied.

Pipette solutions

For whole-cell recordings we used the following solution (in mM): 125 potassium methylsulfate, 4 ATP-Mg_2, 10 NaCl, 0.3 GTP, 16 $KHCO_3$ plus biocytin (2.5–5 mg ml^{-1}) equilibrated with 95% O_2–5% CO_2 to a pH of 7.3. For cell-attached experiments pipettes were filled with 'recording' ACSF. Unless otherwise specified, control recording ACSF included the following synaptic blockers: NBQX (20 μM), D-AP5 (50 μM) and gabazine (12.5 μM).

Anatomical methods

When the anatomy of the recorded cells was examined after the recording, the slice was quickly transferred to a fixative solution containing 4% paraformaldehyde in 0.1 M phosphate buffer (PB) for at least 48 h and then transferred into 0.1 M PB. Slices were not re-sectioned. Endogenous peroxidase activity was removed by incubating the slices in 1% H_2O_2 in PB solution. Biocytin staining was revealed using 3,3-diaminobenzidine tetrahydrochloride using a standard ABC kit (Vector Laboratories). The axon and dendrite visualization was improved using PB solution containing $(NH_4)_2Ni(SO_4)_2$ (0.0002–0.0004%) and $CoCl_2$ (0.0002%). The slices were then mounted using an aqueous mounting medium (Vectashield; Vector Laboratories), and visualized at 40× magnification, and traced with a microscope-attached camera lucida.

Drugs

Drugs were from: Ascent Scientific (D-AP5, NBQX and gabazine), Sigma Aldrich (AMD3100, BAPTA-AM biocytin, bumetanide, $CsCl_2$ and tetraethylammonium (TEA)), PeproTech (Murine CXCL12), Tocris bioscience (iberiotoxin and paxillin), and Immuno Diagnostic (recombinant human T-cell receptor sCD4, recombinant HIV-1 IIIB glycoprotein gp120). For experiments requiring CD4 priming of gp120 (the association rate constant is slow; see Myszka *et al.* 2000), the two components were pre-incubated for longer than 1 h and added to the recording solution at the same concentration (200 pM, Tran *et al.* 2005).

CXCL12 was used at a concentration (50 nM) that is very effective in dramatically suppressing spontaneous firing activity (Marchionni *et al.* 2010). Although the reported binding affinity of CXCL12 for CXCR4 is one order of magnitude lower (K_d ∼2–4 nM, Crump *et al.* 1997; Balabanian *et al.* 2005; Burns *et al.* 2006), it needs to be considered that the real effective concentration of CXCL12 is also determined by the scavenger activity of CXC chemokine receptor 7 (CXCR7; Naumann *et al.* 2010), which is expressed by Cajal–Retzius cells (Schönemeier *et al.* 2008; Tiveron *et al.* 2010). Apart from in Fig. 11, we used gp120 at a concentration of 200 pM, which has been

shown to saturate calcium responses directly measured both in hippocampal cell cultures and retinal ganglion cells (Dreyer *et al.* 1990; Medina *et al.* 1999). Furthermore, this concentration matches well the order of magnitude of gp120 measured in the serum (∼100–767 pM, Oh *et al.* 1992) and plasma (∼4–130 pM, Rychert *et al.* 2010) of HIV-infected individuals.

Statistical methods and analysis of CXCL12/gp120 effects

Statistical analysis was performed using the following software packages: Clampfit 9.0, Excel, Origin and Prism (Graphpad, San Diego, CA, USA). Data are presented as mean ± SEM. Paired *t* tests were employed and the significance level was set at 0.05.

For cell-attached experiments, the effect of CXCL12 (or gp120) was evaluated following application of the chemokine by measuring firing properties in the first minute occurring after wash out of CXCL12 (or gp120, $t = 4$–5 min from the start), and compared with the first minute of baseline at the beginning of the recordings ($t = 0$–1 min from the start, see shadings in Fig. 3). The reason for the choice of this time interval is that the effects of CXCL12 and gp120 are relatively slow to develop, persist after their wash-out and the selected time window is a good compromise between steady state of the CXCL12-induced effect and the peak response to gp120. Furthermore, and more importantly, CXCL12 completely eliminated action currents in some cells. Therefore, choosing a later time point closer to steady state would have significantly reduced the number of recordings that could be used for statistical testing of the action currents amplitudes. For experiments including neurons that stopped firing during the time window used for the analysis of the effect of CXCL12, the number of cells that became silent is explicitly mentioned in the text. In the other experiments where this is not mentioned, firing persisted in the time windows used for the analysis in all cells. Amplitude of the action currents was calculated from the positive to the negative peak of the waveform. The frequency of the action currents was calculated based on the time of their negative peaks.

For whole-cell recordings, the effect of gp120 was evaluated during the first 2 min immediately following application of the protein ($t = 13$–15 min from breakthrough, see shading in Fig. 8). In these experiments a 2 min control period was selected after reaching equilibrium following the breakthrough-dependent hyperpolarization ($t = 8$–10 min from breakthrough, see shading in Fig. 8).

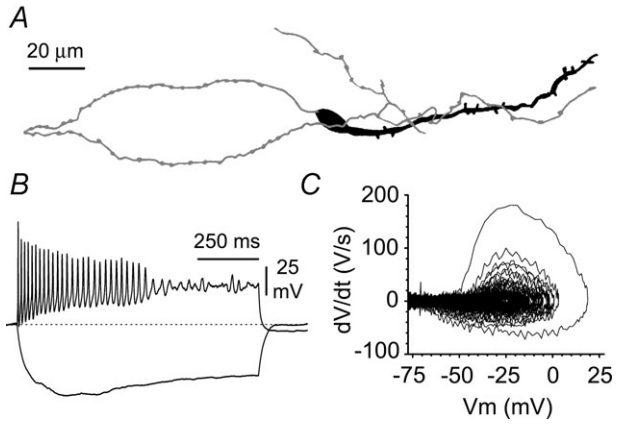

Figure 1. Basic characteristics of hippocampal Cajal–Retzius cells of the CXCR4-EGFP mouse
A, stereotypical appearance of an EGFP-expressing Cajal–Retzius cell of CA1 stratum lacunosum-moleculare (Marchionni *et al.* 2010). Notice the tadpole-like morphology (soma/dendrite: black, axon: grey). *B*, basic electrophysiological properties of Cajal–Retzius cells. Notice the rapidly decreasing amplitude of the spikes with membrane depolarization and the sag elicited by hyperpolarizing current injections (pulses were +60 pA and −25 pA, respectively, 1 s duration). *C*, phase plot of the record shown in *B* illustrating the rapidly decreasing d*V*/d*t* at more depolarizing potentials.

Results

The purpose of this study was to investigate CXCR4-dependent modulation of membrane excitability in Cajal–Retzius cells by physiological and pathological ligands, namely the chemokine CXCL12 and the HIV-1 envelope glycoprotein gp120.

When recorded in whole-cell configuration and held hyperpolarized, hippocampal Cajal–Retzius cells have a characteristic firing patterns and membrane properties (Fig. 1; see also Marchionni *et al.* 2010). However, the study of membrane excitability in whole-cell conditions is technically problematic because whole-cell configuration imposes on these cells a non-physiological hyperpolarized resting state (Mienville & Pesold, 1999; Marchionni *et al.* 2010). The experiments of Fig. 2 confirm, once again (compare with Fig. 11*A* of Marchionni *et al.* 2010), that the depolarized membrane potential initially measured in Cajal–Retzius cells is rapidly lost after breakthrough. The averaged membrane potential measured in the first 2 min ($t = 0$–2 min) after breakthrough was -45 ± 1 mV *vs.* -63 ± 2 mV measured after reaching steady state ($t = 8$–10 min, $P < 0.05$, $n = 11$). The sensitivity of this cell type to whole-cell recording is most parsimoniously explained by its relatively small cytoplasmic volume and simple dendritic structure, which is likely to be particularly vulnerable to alterations of intracellular components associated with sustaining firing.

Therefore, we decided to study spontaneous firing by monitoring action currents recorded in the less invasive cell-attached configuration. In addition, we considered the

amplitude of the action currents as a proxy for the state of depolarization of the membrane. In fact, as shown in Fig. 1 (see also Marchionni *et al.* 2010), the amplitude of the action potential of Cajal–Retzius cells is exquisitely sensitive to the polarization state of the membrane, most probably because of sodium channel inactivation.

Before addressing pharmacologically the conductance(s) responsible for CXCL12-induced modulation of firing, we designed an initial set of experiments to confirm both the stability of our recording conditions and that CXCL12-dependent modulation is independent of the presence/absence of synaptic blockers. As shown in Fig. 3, in the presence of synaptic blockers (20 μM NBQX, 50 μM D-AP5 and 12.5 μM gabazine), both spontaneous firing frequency and spike amplitude remained stable, further validating the use of cell-attached *vs.* whole-cell configuration. The frequency of spontaneous firing was 6.5 ± 0.7 Hz at the beginning of the recording ($t = 0$–1 min) *vs.* 6.5 ± 1.5 Hz at a later time point ($t = 4$–5 min, $P > 0.05$, $n = 6$ (for the reasons underlying the selection of this specific time point see Methods)). The amplitude of action currents in the same time periods was 24 ± 2 pA and 24 ± 2 pA, respectively ($n = 6$, $P > 0.05$).

Application of CXCL12 (50 nM) rapidly and dramatically reduced tonic firing, both in the presence (as previously reported by Marchionni *et al.* 2010, compare with their Fig. 10*B*), and in the absence of synaptic blockers. In the presence of synaptic blockers CXCL12 decreased action current frequency from 6.0 ± 01.4 Hz to 0.9 ± 0.7 Hz ($P < 0.05$, $n = 10$), whereas in drug-free ACSF the firing frequency declined from 6.7 ± 01.8 Hz to 2.2 ± 1.1 Hz ($P < 0.05$, $n = 8$). As expected, the few action currents remaining after CXCL12 application were of larger amplitude than the ones recorded in control conditions, consistent with the membrane hyperpolarization reported by Marchionni *et al.* (2010). In the presence of synaptic blockers the amplitude of action currents increased from 26 ± 5 pA to 33 ± 4 pA ($n = 6$, the remaining four cells had already completely stopped firing in this time period and no action currents could be detected, $P < 0.05$). When CXCL12 was applied in the absence of synaptic blockers, action current amplitudes increased from 30 ± 12 pA to 41 ± 15 pA, before and after the addition of the chemokine, respectively ($P < 0.05$, $n = 8$).

Having clarified these preliminary points, we asked what intrinsic conductance mediates the response to CXCL12.

Because our previous work (Marchionni *et al.* 2010) had indicated that reduced firing activity is mediated by membrane hyperpolarization associated with an increased conductance, we designed experiments aimed to test the possible involvement of potassium channels. In particular, given that CXCR4 belongs to the superfamily of G protein-coupled receptors, we began by testing the possible involvement of potassium inward rectifier channels, which have been shown to be directly regulated by several other receptors belonging to this superfamily (Isomoto *et al.* 1997).

As shown in Fig. 3, in the constant presence of cesium (2 mM), which at this external concentration blocks inward rectifying potassium channels (Sodickson & Bean, 1996), application of CXCL12 still affected both firing frequency (5.5 ± 0.6 Hz in control solution *vs.* 1.0 ± 0.4 Hz after CXCL12 application, $n = 6$, $P < 0.05$) and action potential amplitude (24 ± 3 pA before *vs.* 36 ± 3 pA after the

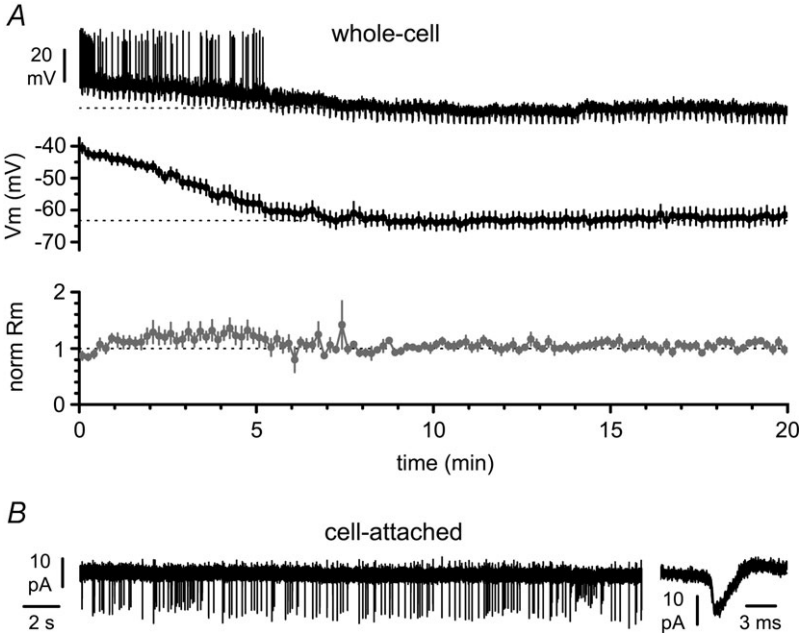

Figure 2. Cajal–Retzius cells are particularly sensitive to whole-cell recording conditions
A, top panel: a spontaneously firing Cajal–Retzius cell loses its spontaneous activity after breakthrough (beginning of the trace, $t = 0$ min) and acquires a membrane resting potential. Downward deflections are the responses to regularly injected hyperpolarizing current pulses to monitor the membrane input resistance (−5 pA, 1.5 s duration). Middle panel: summary plot from several experiments showing a robust hyperpolarization occurring within the first ∼5 min from breakthrough. Lower panel: summary graph of the estimated membrane input resistance (Rm). *B*, spontaneous firing monitored in cell-attached recording configuration. Notice the presence of action currents shown at slower (left panel) and faster (right panel) time scales.

addition of the chemokine, $P < 0.05$, $n = 5$, one cell had already stopped firing during the time window selected for these measurements). Therefore, we concluded that inward rectifying potassium channels were not responsible for CXCL12-induced modulation.

Next, we considered that CXCL12 has been shown to trigger intracellular calcium release in a variety of cells types (Guyon & Nahon, 2007), and therefore decided to test the possibility that CXCL12 acted by increasing a calcium-dependent potassium conductance (Fig. 4). If this were the case, then responses to CXCL12 should be strongly reduced both by intracellular calcium chelation and by blockers of calcium-dependent potassium channels. When slices were pre-treated with BAPTA-AM (see Methods for details), the frequency of spontaneous firing changed from 6.1 ± 1.0 Hz in control solution to 4.2 ± 0.7 Hz after bath perfusion of CXCL12 ($n = 9$, $P > 0.05$). The amplitude of the action currents did not change either (baseline value: 22 ± 3 pA *vs.* 21 ± 3 pA post CXCL12 application, $n = 9$, $P > 0.05$), consistent with the idea that CXCL12-induced modulation depends on an increase in intracellular calcium levels.

To corroborate the interpretation of this result as evidence for the involvement of calcium-dependent potassium channels in mediating CXCL12-dependent modulation, we tested the effect of treatments known

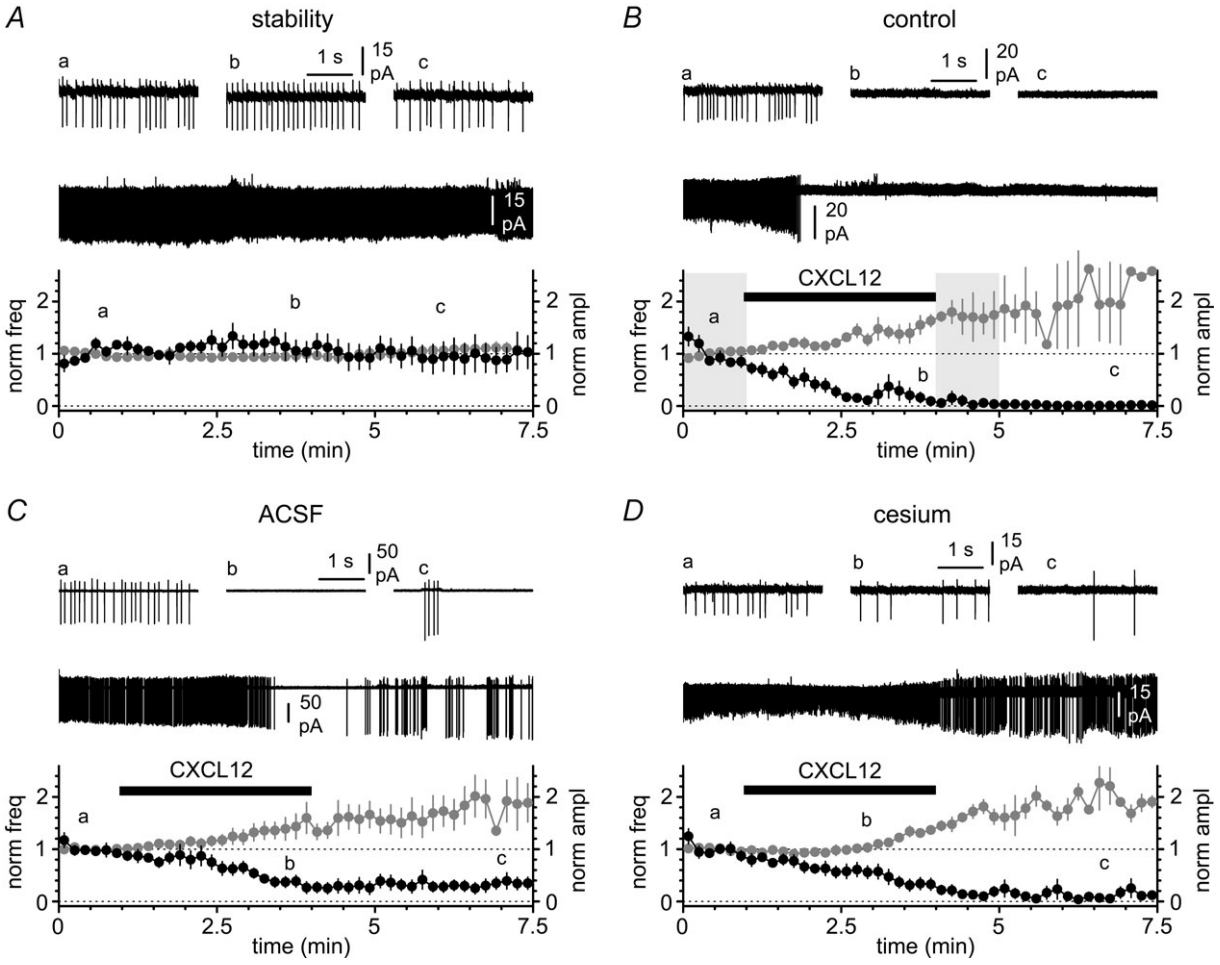

Figure 3. Modulation of spontaneous firing by CXCL12 application in cell-attached conditions
A, spontaneous firing can be monitored by measuring the frequency (black circles) and amplitude (grey circles) of the action currents. Notice that in the absence of CXCL12 application both parameters remain stable in control solution (ACSF + synaptic blockers). Insets show the entire recording and selected portions at different time points (a, b and c). *B*, application of CXCL12 (black bar, 50 nM) dramatically decreases the frequency of the action currents and concomitantly increases their amplitude. Insets illustrate the entire recording and selected portions before the application of CXCL12 (a), in its presence (b) and after its removal (c). Notice that the effect is long-lasting. The shaded areas indicate the time windows used for the quantification of firing frequency and action current amplitude in control and after modulation by the chemokine (see Methods). *C*, as in *B*, but experiments were performed in the absence of synaptic blockers. Notice the persistence of a strong effect both on frequency and amplitude. *D*, as in *A* and *B*, but in the constant presence of extracellular cesium (2 mM), to test the involvement of potassium inward rectifiers in the response produced by CXCL12. Notice the persistence of the effect.

to block the large-conductance calcium-dependent potassium channel, BK, which is expressed by Cajal–Retzius cells (Mienville, 1998).

In the constant presence of TEA at low concentrations (1 mM, known to block BK channels, see Iwatsuki & Petersen 1985), firing frequency was 3.7 ± 0.8 Hz in control conditions compared with 3.6 ± 0.9 Hz after the addition of CXCL12 ($n = 6$, $P > 0.05$). The amplitude of the action currents remained also unchanged (24 ± 3 pA *vs.* 23 ± 3 pA before and after perfusion with the chemokine, respectively, $n = 6$, $P > 0.05$).

The response to CXCL12 was similarly prevented by more specific blockers of BK channels. When paxilline (10 μM) was added to the control external solution, the firing frequency was 4.2 ± 0.5 Hz *vs.* 3.6 ± 0.8 Hz before and after the exposure of the slice to CXCL12, respectively ($P > 0.05$, $n = 7$). The amplitude of the action currents was 23 ± 3 pA during the initial baseline compared with 21 ± 3 pA after perfusion of CXCL12 ($n = 7$, $P > 0.05$).

Lastly, we tested the effects of iberiotoxin (100 nM). In the constant presence of the toxin, spontaneous firing was 6.1 ± 1.3 Hz and 6.3 ± 1.6 Hz before and after the addition of CXCL12, respectively ($n = 5$, $P > 0.05$). The amplitude of the observed action currents was 35 ± 6 pA *vs.* 30 ± 6 pA ($n = 5$, $P > 0.05$).

This battery of experiments demonstrates that reduced excitability following CXCL12 exposure is due to the increase of a calcium-dependent potassium conductance specifically mediated by BK channels. This is consistent with the CXCR4-dependent modulation of BK channels, which has been reported in other preparations (Florio *et al.* 2006).

Next, we wondered whether the firing frequency before drug application was related to the magnitude of the

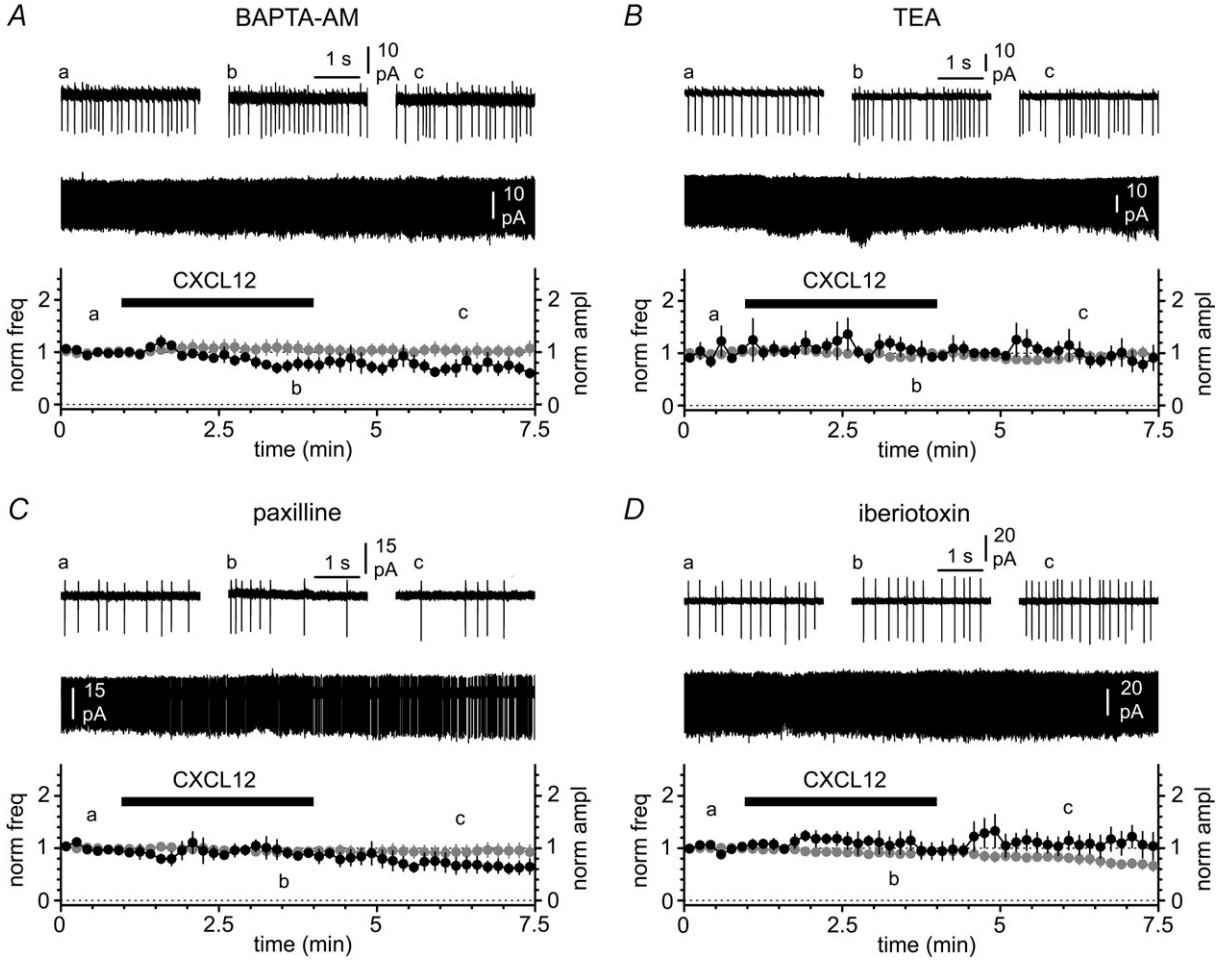

Figure 4. Modulation of spontaneous firing by CXCL12 is mediated by BK-type calcium-activated potassium channels
A, lack of effects on frequency and amplitude of action currents when CXCL12 is applied (black bar, 50 nM) to slices pre-conditioned by BAPTA-AM. Insets illustrate the entire recording and selected portions before the application of CXCL12 (a), in its presence (b) and after its removal (c). *B*, *C* and *D*, as in *A*, but in the constant presence of TEA (1 mM), paxilline (10 μM) and iberiotoxin (100 nM), respectively. Notice that all these blockers of BK channels prevent the effect of CXCL12.

observed effects. As shown in the summary plots of Fig. 5, no obvious relation was observed between the initial frequency and the magnitude of CXCL12-induced modulation. Similarly, the blocking effect of the various pharmacological treatments did not appear to depend on the original firing frequency measured before CXCL12 application. This observation indicates that the increase of BK channel activity is powerful enough to reduce excitability even in the most active cells of our sample.

Having identified BK channels as effectors of CXCL12-triggered modulation, we next considered that, under the appropriate conditions, the HIV-1 envelope glycoprotein gp120 can act as a functional agonist for CXCR4 and also produce intracellular calcium responses in neurons (Lo *et al.* 1992). Therefore, we tested this possibility by applying gp120 to slices while monitoring the activity of Cajal–Retzius cells (Fig. 6). We used a concentration (200 pM) that has been shown to saturate calcium responses directly measured both in hippocampal cell cultures and retinal ganglion cells (Dreyer *et al.* 1990; Medina *et al.* 1999). Furthermore, this concentration matches well the order of magnitude of gp120 measured in the serum (∼100–767 pM, Oh *et al.* 1992) and plasma (∼4–130 pM, Rychert *et al.* 2010) of HIV-infected individuals. Superfusion of external solution containing gp120 resulted in increased excitability (firing frequency increased from 5.8 ± 0.9 Hz to 8.5 ± 1.1 Hz after the addition of the protein, $n = 19$, $P < 0.05$) associated with reduced amplitude of action currents (amplitude was 39 ± 5 pA in control *vs.* 28 ± 3 pA after application of gp120, $n = 19$, $P < 0.05$).

Binding of gp120 to the CXCR4 receptor often (but not always: for CD4-independent association between HIV-1 gp120 and CXCR4 see Hesselgesser *et al.* 1997) requires conformational changes induced by the surface glycoprotein CD4 (Sattentau & Weiss, 1998), which is typically expressed by thymocytes and a subset of T lymphocytes. Therefore, we compared the effects of primed gp120 (by pre-incubation, see Methods) to the one observed following application of gp120 alone. Modulation caused by gp120/CD4 was very similar to the one triggered by gp120 in the absence of CD4. Spontaneous firing frequency increased from 4.7 ± 0.7 Hz to 7.7 ± 1.5 Hz after addition of gp120/CD4 ($n = 10$, $P < 0.05$). Action current amplitude concurrently decreased from 39 ± 3 pA to 26 ± 2 pA ($n = 10$, $P < 0.05$). These results confirm that the CD4 dependence of gp120–CXC4 interaction is cell-type specific (Bodner *et al.* 2003) and, apparently, is not involved in the phenomenon described here.

To further strengthen our interpretation that the observed effects were mediated by CXCR4, we applied gp120 to slices exposed to the CXCR4 antagonist AMD3100 (1 μM; Fig. 6*C*). The presence of the antagonist fully prevented gp120-induced modulation of firing, confirming our conclusion that this was a CXCR4-specific effect. Firing frequency did not increase, but was actually slightly reduced from 8.0 ± 1.5 Hz to 6.7 ± 1.3 ($n = 11$, $P < 0.05$), and no significant changes could be detected in the amplitude of action currents (from 29 ± 2 pA to 27 ± 2 pA, respectively, $n = 11$, $P > 0.05$). Lastly, because (at the developmental stage we used) Cajal–Retzius cells are the only neuron of stratum lacunosum-moleculare expressing CXCR4, we monitored the cell-type specificity of the effects of gp120. When recordings were performed from EGFP-negative local interneurons, spontaneous action currents were not observed either before or after application of gp120 ($n = 4$, data not shown). Therefore, we performed the following experiments after raising extracellular KCl to 7–10 mM. Under these modified experimental conditions, firing frequency was 5.3 ± 1.0 Hz before application of the protein and 5.3 ± 1.1 Hz after its addition to the external solution ($n = 9$, $P > 0.05$). The amplitude of action currents was also unaffected (control: 114 ± 27 pA *vs.* 121 ± 31 pA in gp120, $n = 9$, $P > 0.05$). These results are consistent with the reported selective expression of CXCR4 by Cajal–Retzius cells, within the population of

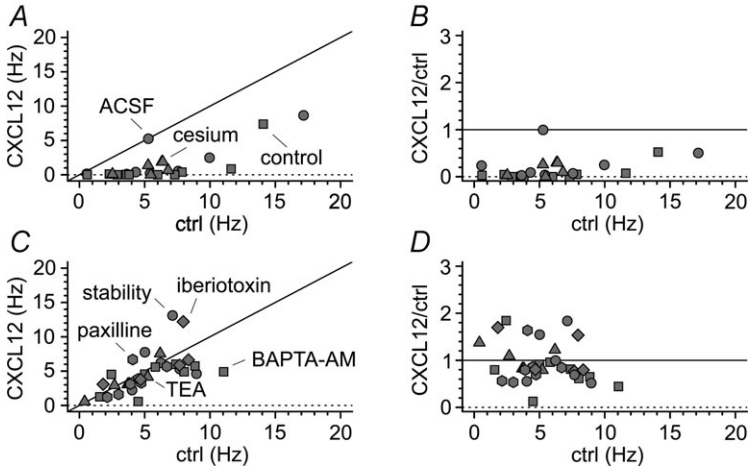

Figure 5. Plots of individual results from several CXCL12 experiments and stability test
A, summary graph illustrating frequencies of spontaneous firing before (ctrl) and after the application of CXCL12 (CXCL12). Notice that application of the chemokine in control solution (squares), ACSF (circles) or in the constant presence of cesium (triangles) results in almost all the experiments in frequencies below the identity line (black line). *B*, normalized effect of CXCL12 application on spontaneous frequencies under the same experimental conditions as in *A*. Notice that frequency is strongly decreased irrespective of the frequencies measured before CXCL12 application. *C* and *D*, as in *A* and *B*, respectively, but for experiments in which no modulation of firing is present (stability: circles, BAPTA-AM: squares, TEA: triangles, paxilline: hexagons, iberiotoxin: diamonds). Notice the individual data points in *C* clustering around the identity line, and the lack of normalized effects in *D*.

stratum lacunosum-moleculare neurons of juvenile/adult animals (Stumm *et al.* 2002; Marchionni *et al.* 2010).

Overall, these findings indicate that gp120 produces CXCR4-dependent functional effects in Cajal–Retzius cells, but of opposite direction compared with the ones generated by its physiological ligand, CXCL12. The absence of the requirement of CD4 priming also confirms that CD4 and/or proteins with similar functions are likely to be expressed in the nervous tissue (Omri *et al.* 1994; Bodner *et al.* 2003, however, see also Hesselgesser *et al.* 1997 for CD4-independent association between gp120 and CXCR4).

When we examined the data in more detail, another difference between the effects of CXCL12 and gp120 (and gp120/CD4) emerged. As shown in the summary plots of Fig. 7, the increase of firing frequency appeared to be much stronger in cells with initial low spontaneous firing frequencies, suggesting that the conductance that is modulated by gp120 may be already fully saturated in the more active cells. In contrast, and as expected, the effect of AMD3100 did not appear to depend on the initial firing rate.

How does the gp120–CXCR4 interaction lead to the increase in spontaneous firing? As already mentioned, whole-cell conditions severely reduce successful responses to application of CXCL12 (only ∼50% of the cells recorded under this configuration respond to the chemokine, see Marchionni *et al.* 2010), which is consistent with washout of responses from intracellular calcium stores. We reasoned that, if the gp120–CXCR4 pathway involved a

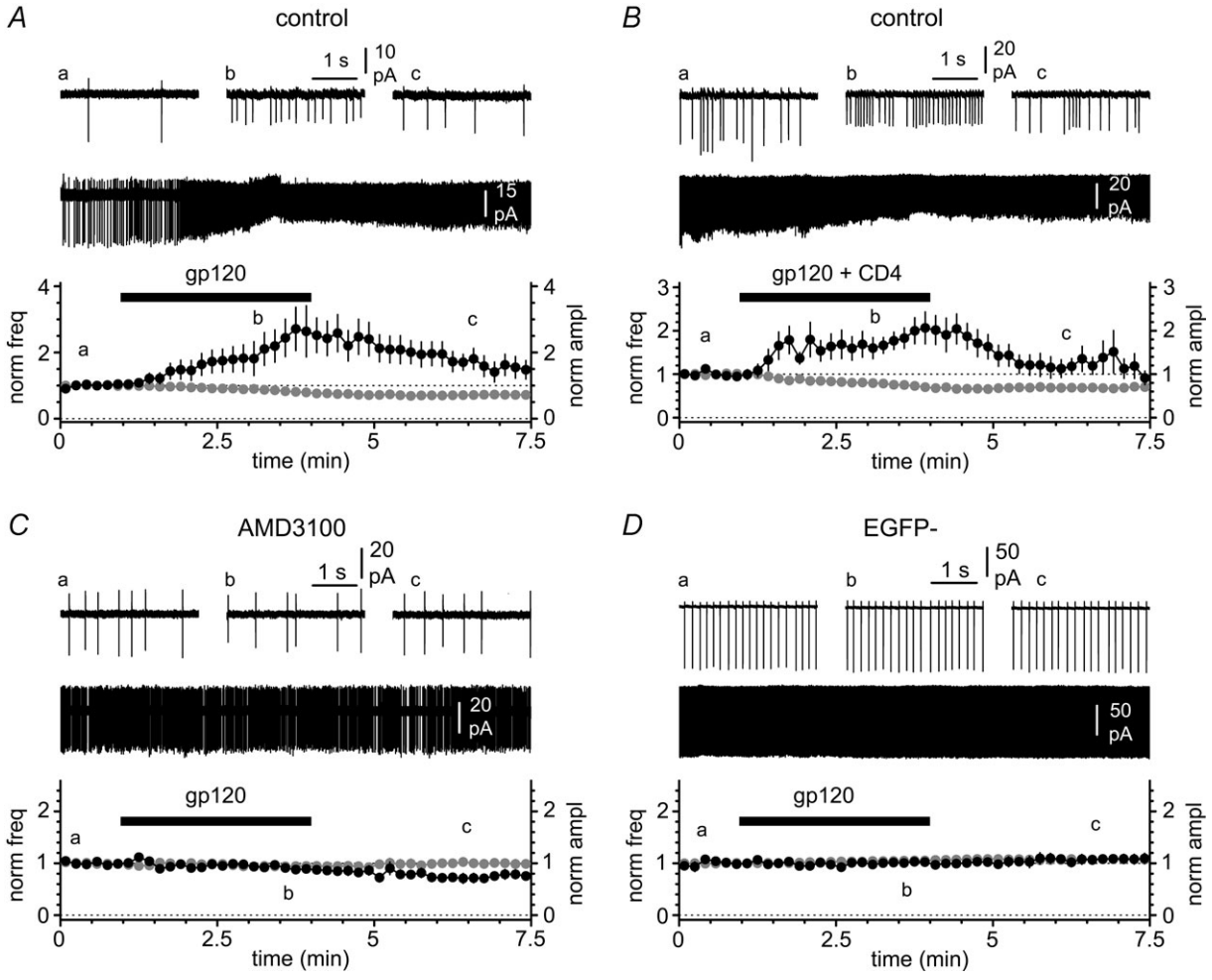

Figure 6. gp120 increases the excitability of Cajal–Retzius cells via the chemokine receptor CXCR4 in an apparent CD4-independent fashion
A, application of gp120 (black bar, 200 pM) increases spike frequency and decreases the amplitude of the action currents. Insets illustrate the entire recording and selected portions before the application of gp120 (a), in its presence (b) and after its removal (c). *B*, as in *A*, but gp120 was primed with equimolar CD4. Notice the similarity of the effects on frequency and amplitude compared to gp120 alone in *A*. *C*, as in *A* and *B*, but in the presence of the CXCR4 antagonist AMD3100 (1 μM). Notice that the antagonist prevents the gp120-induced modulation. *D*, as in the previous panels, but recordings were made from stratum EGFP non-expressing neurons in stratum lacunosum-moleculare. Notice the absence of any effect induced by gp120.

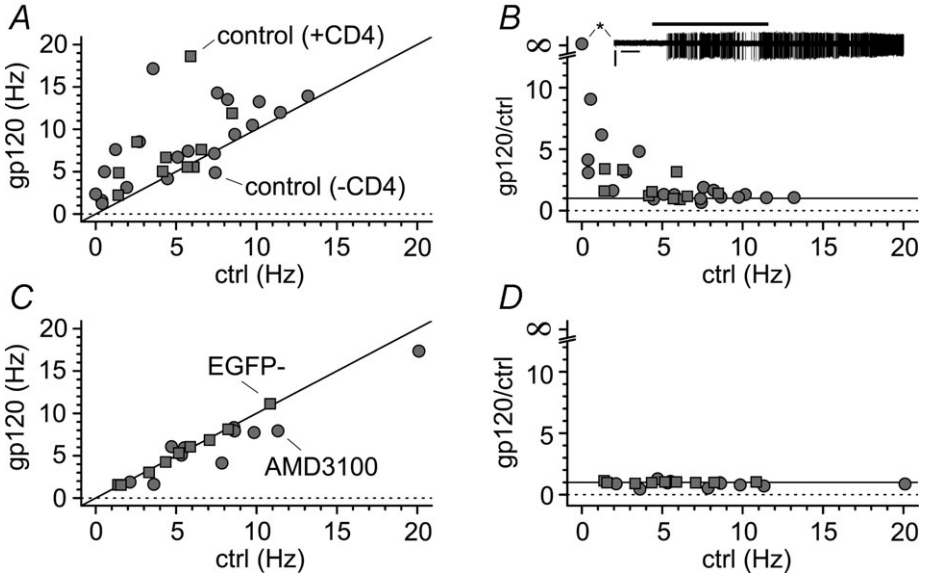

Figure 7. The increased excitability caused by gp120 appears to be frequency dependent
A, plot of results from individual experiments (gp120 alone: control, grey circles; gp120 primed and in the constant presence of CD4: CD4, grey squares). Notice the scatter of the data above the identity line (black line). *B*, normalized effect of gp120 application on spontaneous frequencies under the same experimental conditions as in *A*. Notice that the effect of gp120 is much stronger when tested on cells with low control frequencies. The inset (asterisk) shows that gp120 application could trigger firing in a resting Cajal–Retzius cell. *C* and *D*, as in *A* and *B*, respectively, but for experiments where the effect of gp120 was either blocked by the CXCR4 antagonist AMD3100 (grey circles) or absent (EGFP non-expressing cells: $EGFP^-$, grey squares). Notice the clustering of the data around the identity line and the lack of effects independent of the control frequency.

different transduction/effector mechanism, then it might be less sensitive to whole-cell conditions, and allow the direct monitoring of changes in membrane potential and input resistance.

However, when we applied gp120 to Cajal–Retzius cells recorded under whole-cell conditions (Fig. 8), we were unable to detect any change in either membrane potential or input resistance. After steady state was reached, the membrane potential was -56 ± 4 mV (time 8–10 min from breakthrough), which compared with -55 ± 4 mV after gp120 application (time 13–15 min from breakthrough, $n = 10$, $P > 0.05$). In the same periods, cell input resistance was 1.2 ± 0.2 GΩ *vs.* 1.3 ± 0.2 GΩ, respectively ($n = 10$, $P > 0.05$). This result indicates that the signal transduction/effector mechanisms underlying gp120 functional effect is as sensitive, if not more, to loss of cytoplasmic components, similarly to the CXCL12-dependent pathway (Marchionni *et al.* 2010).

One possibility to explain these results is that gp120 also triggers intracellular calcium responses, similarly to CXCL12 (Lo *et al.* 1992; Meucci *et al.* 1998; Medina *et al.* 1999; Khan *et al.* 2004). Therefore, we performed gp120 applications on slices transiently pre-incubated with BAPTA-AM (Fig. 9). In order to avoid negative results due

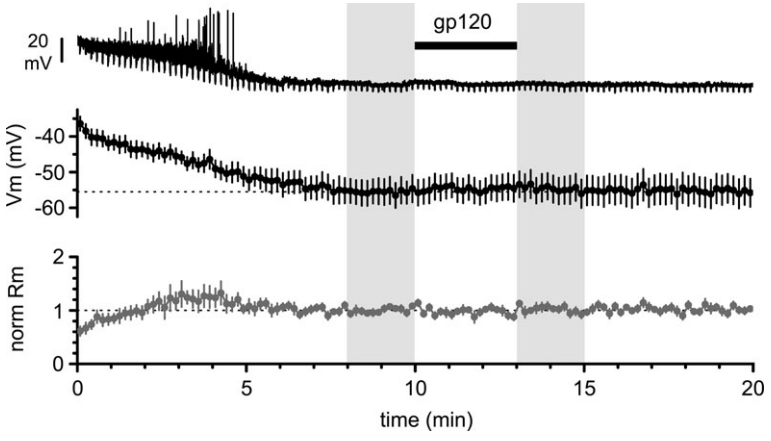

Figure 8. The effects of gp120 are lost when whole-cell recording conditions are used
Top panel: original recording from a Cajal–Retzius cell, which progressively hyperpolarizes its membrane potential following breakthrough (beginning of the trace, $t = 0$ min). Downward deflections are the responses to regularly injected hyperpolarizing current pulses to monitor the membrane input resistance (−5 pA, 1.5 s duration). Middle panel: summary plot from several experiments showing a total lack of effect of gp120 application (200 pM, black bar). Lower panel: summary graph of the estimated membrane input resistance. The shaded areas indicate the time windows used for the quantification of membrane potential and cell input resistance in control and after application of gp120.

to spontaneous high-frequency firing in the sample, we recorded for this experiment from pre-selected cells that were active at low tonic rates. Under these experimental conditions, firing frequency was 3.3 ± 0.5 Hz before gp120 application and 2.6 ± 0.4 Hz after its addition ($n = 14$, $P > 0.05$). Similarly, the amplitude of peak action currents did not change and was 37 ± 7 pA in control *vs.* 36 ± 6 pA after perfusion of the chemokine in the bath ($n = 14$, $P > 0.05$). Therefore, we concluded that gp120-dependent modulation of spontaneous activity also requires changes in intracellular calcium levels.

How can activation of the same receptor lead to opposite results mediated by the same pathway? Direct study of intracellular calcium responses induced by CXCL12 and gp120 in neurons (Meucci *et al.* 1998), neuronal progenitors (Tran *et al.* 2005) or cell lines (Khan *et al.* 2004) has shown that both types of agonist can produce calcium transients. However, one possibility is that CXCL12 and gp120 possess different intrinsic efficacy (Clarke & Bond, 1998) for calcium responses and hence generate distinct free calcium levels. Alternatively, specific agonists could trigger calcium release from distinct calcium pools that affect specific conductances. Our data show that we have used doses of CXCL12 that were able to recruit BK channels, which increase their own activity at supramicromolar calcium concentrations (Womak & Khodakhah, 2002; Qian *et al.* 2006). One possible explanation, therefore, would posit that application of gp120 triggers weaker calcium peaks (or elicits responses that are spatially distant/segregated from BK channels), but which are nevertheless able to affect some other calcium-sensitive conductances with a lower calcium threshold (or with a more favourable localization). Calcium-dependent chloride channels are activated by calcium in the submicromolar range (Caputo *et al.* 2008) and inhibited at supramicromolar calcium concentrations (Fuller *et al.* 1994). Thus, according to this possibility, strong calcium responses would predominantly affect BK channels, whereas a weaker calcium level would activate calcium-sensitive chloride channels. Because of the lack of expression of the KCC2 transporter in Cajal–Retzius cells (Pozas *et al.* 2008), an increased chloride conductance would be predicted to enhance excitability. However, the lack of a selective pharmacology for calcium-activated chloride channels prevented us from interfering specifically with these types of channels because currently available blockers suffer from many unrelated side effects (Hartzell *et al.* 2005). Therefore, we decided to test the involvement of a chloride conductance by manipulating the electrochemical gradient for chloride. We used bumetanide to block the $Na^+,K^+,2Cl^-$ type I cotransporter (NKCC1), which is necessary to maintain elevated intracellular chloride concentrations in Cajal–Retzius cells (Achilles

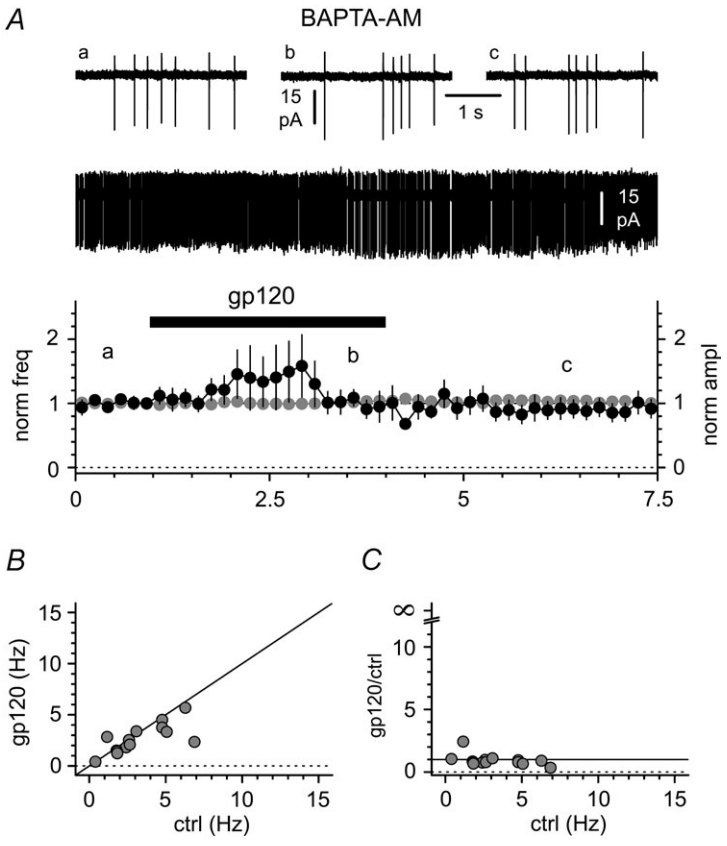

Figure 9. gp120-induced modulation of activity in Cajal–Retzius cells depends on intracellular calcium
A, application of gp120 (200 pM, black bar) to slices conditioned by BAPTA-AM does not change either spontaneous firing frequency or action current amplitude. Insets illustrate the entire recording and selected portions before the application of gp120 (a), in its presence (b) and after its removal (c). *B*, the lack of effect in BAPTA-AM-treated slices is not due to frequency-dependent effects. The summary plot of the individual results shows that for this experiment we pre-selected cells with low control firing rates. Notice the clustering of the data around the identity line (black line). *C*, the lack of effect is apparent in a frequency range that is associated with increased excitability in non-conditioned slices (compare this panel with Fig. 7*B*).

et al. 2007). Exposure of slices to the NKCC1 blocker bumetanide (50 μM, pre-incubated for at least 30 min and constantly present during the experiment) was indeed able to prevent the increase of firing frequency caused by gp120 (Fig. 10). Under these experimental conditions, firing frequency was 5.8 ± 0.8 Hz before gp120 application *vs.* 4.6 ± 1.2 Hz after its addition ($n = 9$, $P > 0.05$); the amplitude of action currents did not change significantly (29 ± 4 pA in control *vs.* 27 ± 5 pA in gp120 ($n = 9$, $P > 0.05$).

The results of these experiments confirm that CXCL12 and gp120 affect the intrinsic firing of Cajal–Retzius cells bi-directionally by acting on different ionic conductances. Taken together with the BAPTA sensitivity of both mechanisms, these data reinforce our hypothesis of a partial agonism (Ahuja & Smith, 2009) at the CXCR4 receptor that could generate calcium responses of different amplitude.

Lastly, although, as we have already mentioned, the concentrations of gp120 used so far (200 pM) have been reported to saturate calcium responses directly measured both in hippocampal cell cultures and retinal ganglion cells (Dreyer *et al.* 1990; Medina *et al.* 1999), an alternative explanation for the discrepant results using CXCL12 *vs.* gp120 could simply be that, in our specific system, 200 pM is not a concentration generating saturating responses. Thus, exposing slices to higher doses of gp120 might produce larger calcium transients, and activate BK channels. If this was the case, higher concentrations of gp120 should result in electrophysiological effects very similar to the one produced by CXCL12.

We decided to test this possibility by exposing slices to gp120 at nanomolar concentrations (1–50 nM). As shown in Fig. 11, the summary plots of the effect of gp120 at nanomolar concentrations were strikingly similar to the plots obtained at 200 pM (compare with Fig. 7), but very different from the results obtained with CXCL12 (compare with Fig. 5). Thus, this last control experiment confirmed that the bi-directional modulation of firing activity was not due to an insufficient dose of gp120. Application of nanomolar levels of gp120 (1–50 nM) increased firing frequency from a control value of 4.1 ± 0.6 Hz to 6.0 ± 0.7 Hz ($n = 25$, $P < 0.05$), and reduced the amplitude of action currents from 47 ± 5 pA to 42 ± 5 pA ($n = 25$, $P < 0.05$).

Discussion

We have demonstrated that CXCR4 expressed by Cajal–Retzius cells can modulate spontaneous firing bi-directionally. CXCL12, which is believed to be the physiological agonist of the receptor, depresses firing rates via BK-subtype calcium-dependent potassium

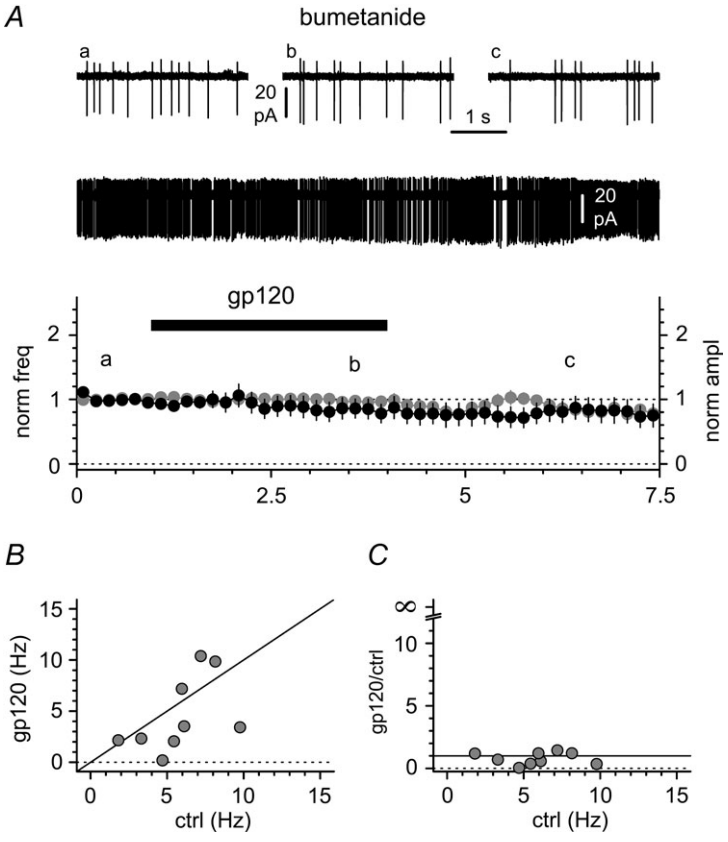

Figure 10. Effect of the NKCC1 blocker bumetanide (50 μM) on gp120-induced modulation of activity in Cajal–Retzius cells
A, application of gp120 (200 pM, black bar) to slices pre-incubated and in the constant presence of bumetanide does not change either spontaneous firing frequency or action current amplitude. Insets illustrate the entire recording and selected portions before the application of gp120 (a), in its presence (b) and after its removal (c). *B*, the lack of effect in bumetanide-treated slices is not due to frequency-dependent effects. The summary plot of the individual results shows that for this experiment we pre-selected cells with low control firing rates. Notice also that in some individual cells gp120 appeared to actually decrease firing frequency (black line = identity line). *C*, the lack of effect is apparent in a frequency range that is associated with increased excitability in non-conditioned slices (compare this panel with Fig. 7*B*).

channels, whereas gp120 increases excitability via a chloride-dependent target, that we suggest is a calcium-activated chloride channel. These results are relevant both for physiological processes and for the understanding of pathological mechanisms of cortical circuit development in the fetus/newborn with congenital HIV-1 infection.

CXCL12 signalling in Cajal–Retzius cells

Our data show that CXCL12 increases intracellular calcium levels, which leads to the recruitment of a BK-type calcium-dependent conductance. The increased BK-type conductance reduces cellular excitability and is often capable of completely blocking spontaneous firing. This sequence of events could be important both at embryonic and postnatal developmental stages for the following reasons.

First, electrical activity is believed to be important during brain development and to play a complementary role to genetic blueprints that determine the wiring of brain circuits (Spitzer, 2006). Recent work has shown a critical link between electrical activity in specific types of migrating interneurons and their correct structural development and positioning in cortical circuits (De Marco García *et al.* 2011). Accordingly, our data suggest that CXCL12-dependent regulation of excitability may contribute to direct the integration of Cajal–Retzius in developing circuits so that they may perform their specific roles. This idea fits very well with previous work showing that CXCL12 acting on Cajal–Retzius cells provides a critical signal for their correct positioning in the developing marginal zone (Borrell & Marín, 2006; Paredes *et al.* 2006).

Although our experiments were performed in postnatal slices, it should be noted that embryonic Cajal–Retzius cells express both BK channels and CXCR4 early in development (Mienville, 1998; Stumm *et al.* 2003). Furthermore, embryonic Cajal–Retzius cells display spontaneous calcium oscillations that are coordinated in specific neuronal assemblies (Aguiló *et al.* 1999), which indicates the early presence of functional action potentials and synaptic transmission. Therefore, the mechanisms we have shown in postnatal Cajal–Retzius cells are very likely to be already operative at earlier developmental stages.

Second, the possibility that the electrical activity of Cajal–Retzius cells may be linked to reelin secretion cannot be completely excluded. In favour of this possibility, Derer *et al.* (2001) suggested axonal secretion of reelin from structures the authors termed 'axonal reelin reservoirs', which would fit very well with axonal activity-dependent regulatory mechanisms. In addition, blocking excitatory serotoninergic projections to Cajal–Retzius cells both pre- and postnatally reduces reelin levels (Janusonis *et al.* 2004; Chameau *et al.* 2009), further suggesting a link between excitability and reelin secretion. Indeed, Cajal–Retzius cells express 5-HT3 serotonin receptors (Chameau *et al.* 2009), which are ligand-gated ion channels and directly affect cellular excitability. However, in different cell types, reelin secretion is likely to follow constitutive pathways (Lacor *et al.* 2000; Tinnes *et al.* 2011).

Third and last, although the number of Cajal–Retzius cells decreases with postnatal maturation (Supèr *et al.* 1998; Chowdhury *et al.* 2010), they do persist in the adult cortex, especially in the hippocampus (of several species: rats, Imamoto *et al.* 1994; Drakew *et al.* 1998; mice, Supèr *et al.* 1998; Alcántara *et al.* 1998; pigs, Abraham *et al.* 2004; humans, Abrahm & Meyer, 2003), where they have been proposed to play computational roles (Marchionni *et al.* 2010; Maccaferri, 2011). Various studies have suggested that they may release an excitatory neurotransmitter, possibly glutamate (Del Rio *et al.* 1995; Radnikow *et al.* 2002; Hevner *et al.* 2003; Soda *et al.* 2003; Ina *et al.* 2007), although no direct evidence of their postsynaptic effect has been yet provided. Assuming that this is the case, CXCL12 activation of a BK

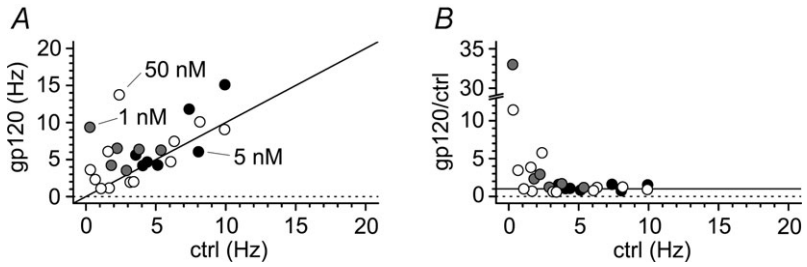

Figure 11. The increase in intrinsic firing of Cajal–Retzius cells is maintained when gp120 is applied in the nanomolar range (1–50 nM)
A, plot of results from individual experiments where gp120 was applied at different nanomolar concentrations (1 nM, grey circles, 5 nM, black circles, 50 nM, white circles). Notice the scatter of the data above the identity line (black line). *B*, normalized effect of gp120 application on spontaneous frequencies under the same experimental conditions as in *A*. Notice that, similarly to what is shown in Fig. 7*B*, the effect of gp120 is much stronger when tested on cells with low control frequencies.

conductance could reduce tonic release of glutamate in stratum lacunosum-moleculare and impact local circuit excitability and direct entorhinal–hippocampal synaptic transmission (Marchionni *et al.* 2010).

From a pathological standpoint, our work has added another potential mechanism of HIV-1 virus-mediated damage to brain development, i.e. dysregulation of Cajal–Retzius cell excitability by gp120. This mechanism should be particularly significant in gestational HIV infections, when the numbers of Cajal–Retzius cells in the developing brain are still very high. If disrupted excitability of Cajal–Retzius cells by gp120 played a role for their migration during early development, then an expected observation would be the presence of ectopic Cajal–Retzius cells in the immature marginal zone of HIV-1-infected fetuses/infants. Intriguingly, this predicted result was part of the neuropathology of fetuses and preterm infants born to HIV-1-positive mothers (Stoltenburg *et al.* 1991), consistent with our proposal. In addition, altered computational functions due to changes in Cajal–Retzius cell excitability could possibly contribute to some of the cognitive deficits of pediatric HIV-1/AIDS. However, given the multiplicity of factors involved (Epstein & Gelbard, 1999), it is difficult to dissect out the potential role of altered excitability of Cajal–Retzius cells *vs.* other mechanisms.

Modulation of excitability in Cajal–Retzius cells by CXCL12 *vs.* gp120

Our data indicate that the activation of the same receptor, CXCR4, by different agonists, CXCL12 and gp120, leads to opposite results i.e. decreased and increased excitability. This bi-directional modulation appears mediated by the same second messenger, intracellular calcium, via different ionic mechanisms (Fig. 12). While our experiments converge to show that several blockers of BK channels effectively prevent CXCL12-induced down regulation of firing, the lack of a reliable specific pharmacology for calcium-activated chloride channels has prevented us using a similar strategy to investigate the conductance regulated by CXCR4 when gp120 is used as an agonist. However, our proposal that a calcium-dependent chloride channel is involved is supported by the results of the bumetanide experiment. In fact, bumetanide-induced blockade of NKCC1 has been estimated to reduce Cajal–Retzius cell intracellular chloride concentrations in the developing neocortex from ∼33 mM to ∼15 mM (Achilles *et al.* 2007). Assuming a similar effect in the postnatal hippocampus, such a shift could abolish or even reverse the effect of gp120 from excitation to inhibition. It is interesting to note that strong inhibition of firing frequency caused by gp120 in the presence of bumetanide was indeed observed in a few cells, although statistical significance for an inhibitory effect in the overall sample tested was not reached. This may depend on the larger variability of responses induced by gp120 when compared with the modulation caused by CXCL12 (compare Fig. 5 with Fig. 7). This difference could suggest that, in some cells, gp120-induced calcium responses are too weak to produce any significant effect, which is also consistent with our general hypothesis.

Furthermore, we would like to highlight that, while the effect of CXCL12 could be recorded in whole-cell conditions in roughly 50% of the cells tested (Marchionni *et al.* 2010), we were never able to see any effect caused by gp120 under identical experimental conditions. This would also be consistent with a weaker calcium response, more vulnerable to whole-cell configuration. Thus, the involvement of a calcium-activated chloride channel with high sensitivity to calcium could also explain the observed frequency dependency of the modulation by gp120. Higher frequency of spontaneous firing would be predicted to be associated with higher intracellular calcium concentrations, which could already activate calcium-dependent chloride channels and hence reduce or even occlude the superimposed effect of gp120. In contrast, lower firing rates would result in lower calcium

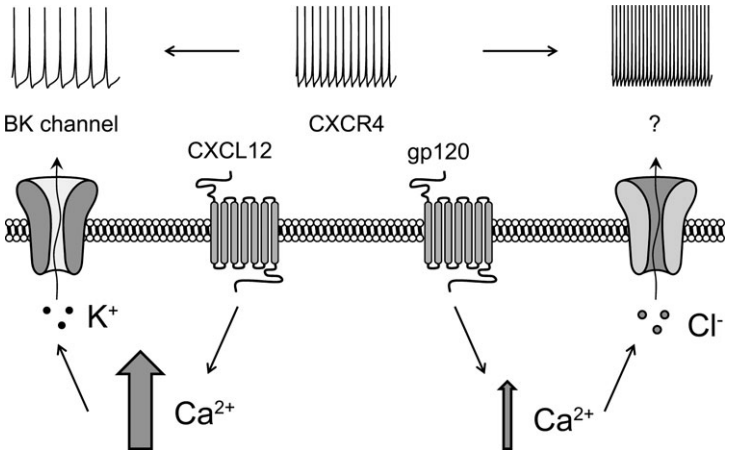

Figure 12. Schematic representation of the proposed hypothesis of biased agonism at the CXCR4 receptor in Cajal–Retzius cells
Activation of CXCR4 by different agonists (CXCL12 *vs.* gp120) leads to quantitatively different intracellular calcium responses (larger *vs.* smaller arrow), which activate specific conductances: BK channels in the case of CXCL12 and a chloride-dependent mechanism in the case of gp120 (here proposed as a calcium-dependent chloride channel, indicated by the question mark). While opening of a potassium conductance leads to reduced excitability, the chloride mechanism modulated by gp120 increases Cajal–Retzius cell spontaneous firing.

levels and allow a wider dynamic range for activation of the calcium-sensitive conductance. All these considerations are consistent with our idea of a different intrinsic efficacy of CXCL12 *vs.* gp120 in generating calcium responses mediated by the CXCR4 receptor.

Different intrinsic efficacies for CXCL12 *vs.* gp120 on CXC4 have been reported also for other signalling pathways and there is an apparent growing number of studies suggesting that the functional effects of gp120 on CXCR4 may be complex and difficult to predict, sometimes similar to the one mediated by CXCL12, other times absent or even opposite (Lazarini *et al.* 2000; see Dwinell *et al.* 2004 *vs.* Xu *et al.* 2011; Khan *et al.* 2004).

Our results suggest that gp120 may act as a partial agonist of CXCR4 expressed by Cajal–Retzius cells. Although a direct demonstration is lacking, we are not the first to propose a partial agonist function for gp120 on the CXCR4 receptor. This is consistent with data showing that gp120 possesses detectable agonist activity for Pyk2 tyrosine kinase in activated CD4-positive T lymphocytes, but results in undetectable intracellular calcium mobilization, which, in contrast, can be clearly measured in the same cells when exposed to CXCL12 (Davis *et al.* 1997). In addition, partial agonism has already been proposed for gp120-triggered calcium responses mediated by CXCR4 in cultured DRG neurons (Oh *et al.* 2001).

Although our results suggest the gp120-dependent involvement of a calcium-activated chloride conductance, we also propose alternative possibilities. For example, calcium could either act on a different, still undetermined, excitatory conductance(s) or electrogenic transporter. Additionally, the two agonists could trigger responses from distinct pools of intracellular calcium, spatially linked to different final effectors. Furthermore, different responses could be due to the binding to the CXCR4 receptor of different G protein subtypes (Kleemann *et al.* 2008) and, lastly, other second messenger systems could be activated concomitantly with intracellular calcium responses, and potentially modulate their strengths.

Further work is needed to conclusively determine the detailed molecular signalling cascade leading to gp120-induced increased excitability.

Conclusions

In summary, our work has revealed novel mechanisms of neuronal regulation mediated by chemokines, which can be disrupted during HV-1 infection and contribute to the manifestations of the disease. We also propose that differences in intrinsic efficacies between CXCL12 and gp120 underlie the opposite CXCR4-dependent bi-directional regulation of Cajal–Retzius cells firing.

References

Abraham H & Meyer G (2003). Reelin-expressing neurons in the postnatal and adult human hippocampal formation. *Hippocampus* **13**, 715–727.

Abraham H, Toth Z & Seress L (2004). A novel population of calretinin positive neurons comprises reelin-positive Cajal–Retzius cells in the hippocampal formation of the adult domestic pig. *Hippocampus* **14**, 385–401.

Achilles K, Okabe A, Ikeda M, Shimizu-Okabe C, Yamada J, Fukuda A, Luhmann HJ & Kilb W (2007). Kinetic properties of Cl uptake mediated by Na^+-dependent K^+-2Cl cotransport in immature rat neocortical neurons. *J Neurosci* **27**, 8616–8627.

Aguiló A, Schwartz TH, Kumar VS, Peterlin ZA, Tsiola A, Soriano E & Yuste R (1999). Involvement of Cajal–Retzius neurons in spontaneous correlated activity of embryonic and postnatal layer 1 from wild-type and reeler mice. *J Neurosci* **19**, 10856–10868.

Ahuja S & Smith SO (2009). Multiple switches in G protein-coupled receptor activation. *Trends Pharmacol Sci* **30**, 494–502.

Alcántara S, Ruiz M, D'Arcangelo G, Ezan F, de Lecea L, Curran T, Sotelo C & Soriano E (1998). Regional and cellular patterns of reelin mRNA expression in the forebrain of the developing and adult mouse. *J Neurosci* **18**, 7779–7799.

Andrade AL & Rossi DJ (2010). Simulated ischaemia induces Ca^{2+}-independent glutamatergic vesicle release through actin filament depolymerization in area CA1 of the hippocampus. *J Physiol* **588**, 1499–1514.

Balabanian K, Lagane B, Infantino S, Chow KY, Harriague J, Moepps B *et al.* (2005). The chemokine SDF-1/CXCL12 binds to and signals through the orphan receptor RDC1 in T lymphocytes. *J Biol Chem* **280**, 35760–35766.

Bodner A, Toth PT, Oh SB, Lu M, Tran PB, Chin RK *et al.* (2003). CD4 dependence of gp120IIIB-CXCR4 interaction is cell-type specific. *J Neuroimmunol* **140**, 1–12.

Borrell V & Marín O (2006). Meninges control tangential migration of hem-derived Cajal–Retzius cells via CXCL12/CXCR4 signaling. *Nat Neurosci* **9**, 1284–1293.

Borrell V, Ruiz M, Del Río JA & Soriano E (1999). Development of commissural connections in the hippocampus of reeler mice: evidence of an inhibitory influence of Cajal–Retzius cells. *Exp Neurol* **156**, 268–282.

Burns JM, Summers BC, Wang Y, Melikian A, Berahovich R, Miao Z *et al.* (2006). A novel chemokine receptor for SDF-1 and I-TAC involved in cell survival, cell adhesion, and tumor development. *J Exp Med* **203**, 2201–2213.

Caputo A, Caci E, Ferrera L, Pedemonte N, Barsanti C, Sondo E *et al.* (2008). TMEM16A, a membrane protein associated with calcium-dependent chloride channel activity. *Science* **22**, 590–594.

Chameau P, Inta D, Vitalis T, Monyer H, Wadman WJ & van Hooft JA (2009). The N-terminal region of reelin regulates postnatal dendritic maturation of cortical pyramidal neurons. *Proc Natl Acad Sci U S A* **106**, 7227–7232.

Chowdhury TG, Jimenez JC, Bomar JM, Cruz-Martin A, Cantle JP & Portera-Cailliau C (2010). Fate of Cajal–Retzius neurons in the postnatal mouse neocortex. *Front Neuroanat* **40**, 10.

Clarke WP & Bond RA (1998). The elusive nature of intrinsic efficacy. *Trends Pharmacol Sci* **19**, 270–276.

Crump MP, Gong JH, Loetscher P, Rajarathnam K, Amara A, Arenzana-Seisdedos F *et al.* (1997). Solution structure and basis for functional activity of stromal cell-derived factor-1; dissociation of CXCR4 activation from binding and inhibition of HIV-1. *EMBO J* **16**, 6996–7007.

Davis CB, Dikic I, Unutmaz D, Hill CM, Arthos J, Siani MA *et al.* (1997). Signal transduction due to HIV-1 envelope interactions with chemokine receptors CXCR4 or CCR5. *J Exp Med* **186**, 1793–1798.

De Marco García NV, Karayannis T & Fishell G (2011). Neuronal activity is required for the development of specific cortical interneuron subtypes. *Nature* **472**, 351–355.

Del Río JA, Heimrich B, Borrell V, Förster E, Drakew A, Alcántara S *et al.* (1997). A role for Cajal–Retzius cells and reelin in the development of hippocampal connections. *Nature* **385**, 70–74.

del Río JA, Martínez A, Fonseca M, Auladell C & Soriano E (1995). Glutamate-like immunoreactivity and fate of Cajal–Retzius cells in the murine cortex as identified with calretinin antibody. *Cereb Cortex* **5**, 13–21.

Derer P, Derer M & Goffinet A (2001). Axonal secretion of reelin by Cajal–Retzius cells: evidence from comparison of normal and Reln(Orl) mutant mice. *J Comp Neurol* **440**, 136–143.

Drakew A, Frotscher M, Deller T, Ogawa M & Heimrich B (1998). Developmental distribution of a reeler gene-related antigen in the rat hippocampal formation visualized by CR-50 immunocytochemistry. *Neuroscience* **82**, 1079–1086.

Dreyer EB, Kaiser PK & Offermann JT & Lipton SA (1990). HIV-1 coat protein neurotoxicity prevented by calcium channel antagonists. *Science* **248**, 364–367.

Drummond GB (2009). Reporting ethical matters in *The Journal of Physiology*: standards and advice. *J Physiol* **587** 713–719.

Dwinell MB, Ogawa H, Barrett KE & Kagnoff MF (2004). SDF-1/CXCL12 regulates cAMP production and ion transport in intestinal epithelial cells via CXCR4. *Am J Physiol Gastrointest Liver Physiol* **286**, G844–G850.

Epstein LG & Gelbard HA (1999). HIV-1-induced neuronal injury in the developing brain. *J Leukoc Biol* **65**, 453–457.

Feng Y, Broder CC, Kennedy PE & Berger EA (1996). HIV-1 entry cofactor: functional cDNA cloning of a seven-transmembrane, G protein-coupled receptor. *Science* **272**, 872–877.

Florio T, Casagrande S, Diana F, Bajetto A, Porcile C, Zona G *et al.* (2006). Chemokine stromal cell-derived factor 1α induces proliferation and growth hormone release in GH4C1 rat pituitary adenoma cell line through multiple intracellular signals. *Mol Pharmacol* **69**, 539–546.

Frotscher M (1998). Cajal–Retzius cells, reelin, and the formation of layers. *Curr Opin Neurobiol* **8**, 570–575.

Frotscher M, Haas CA & Förster E (2003). Reelin controls granule cell migration in the dentate gyrus by acting on the radial glial scaffold. *Cereb Cortex* **13**, 634–640.

Fuller CM, Ismailov II, Keeton DA & Benos DJ (1994). Phosphorylation and activation of a bovine tracheal anion channel by Ca^{2+}/calmodulin-dependent protein kinase II. *J Biol Chem* **269**, 26642–26650.

Guyon A & Nahon JL (2007). Multiple actions of the chemokine stromal cell-derived factor-1α on neuronal activity. *J Mol Endocrinol* **38**, 365–376.

Hartzell C, Putzier I & Arreola J (2005). Calcium-activated chloride channels. *Annu Rev Physiol* **67**, 719–758.

Hesselgesser J, Halks-Miller M, DelVecchio V, Peiper SC, Hoxie J, Kolson DL et al. (1997). CD4-independent association between HIV-1 gp120 and CXCR4: functional chemokine receptors are expressed in human neurons. *Curr Biol 7*, 112–121.

Hevner RF, Neogi T, Englund C, Daza RA & Fink A (2003). Cajal–Retzius cells in the mouse: transcription factors, neurotransmitters, and birthdays suggest a pallial origin. *Brain Res Dev Brain Res* **141**, 39–53.

Imamoto K, Karasawa N, Isomura G & Nagatsu I (1994). Cajal–Retzius neurons identified by GABA immunohistochemistry in layer I of the rat cerebral cortex. *Neurosci Res* **20**, 101–105.

Ina A, Sugiyama M, Konno J, Yoshida S, Ohmomo H, Nogami H *et al.* (2007). Cajal–Retzius cells and subplate neurons differentially express vesicular glutamate transporters 1 and 2 during development of mouse cortex. *Eur J Neurosci* **26**, 615–623.

Isomoto S, Kondo C & Kurachi Y (1997). Inwardly rectifying potassium channels: their molecular heterogeneity and function. *Jpn J Physiol* **47**, 11–39.

Iwatsuki N & Petersen OH (1985). Action of tetraethylammonium on calcium-activated potassium channels in pig pancreatic acinar cells studied by patch-clamp single-channel and whole-cell current recording. *J Membr Biol* **86**, 139–144.

Janusonis S, Gluncic V & Rakic P (2004). Early serotonergic projections to Cajal–Retzius cells: relevance for cortical development. *J Neurosci* **24**, 1652–1659.

Khan MZ, Brandimarti R, Patel JP, Huynh N, Wang J, Huang Z, Fatatis A & Meucci O (2004). Apoptotic and antiapoptotic effects of CXCR4: is it a matter of intrinsic efficacy? Implications for HIV neuropathogenesis. *AIDS Res Hum Retroviruses* **20**, 1063–1071.

Kleemann P, Papa D, Vigil-Cruz S & Seifert R (2008). Functional reconstitution of the human chemokine receptor CXCR4 with G_i/G_o-proteins in Sf9 insect cells. *Naunyn Schmiedebergs Arch Pharmacol* **378**, 261–274.

Lacor PN, Grayson DR, Auta J, Sugaya I, Costa E & Guidotti A (2000). Reelin secretion from glutamatergic neurons in culture is independent from neurotransmitter regulation. *Proc Natl Acad Sci U S A* **97**, 3556–3561.

Lazarini F, Casanova P, Tham TN, De Clercq E, Arenzana-Seisdedos F, Baleux F & Dubois-Dalcq M (2000). Differential signalling of the chemokine receptor CXCR4 by stromal cell-derived factor 1 and the HIV glycoprotein in rat neurons and astrocytes. *Eur J Neurosci* **12**, 117–125.

Lo TM, Fallert CJ, Piser TM & Thayer SA (1992). HIV-1 envelope protein evokes intracellular calcium oscillations in rat hippocampal neurons. *Brain Res* **594**, 189–196.

Maccaferri G (2011). Modulation of hippocampal stratum lacunosum-moleculare microcircuits. *J Physiol* **589**, 1885–1891.

Marchionni I, Takács VT, Nunzi MG, Mugnaini E, Miller RJ & Maccaferri G (2010). Distinctive properties of CXC chemokine receptor 4-expressing Cajal–Retzius cells *versus* GABAergic interneurons of the postnatal hippocampus. *J Physiol* **588**, 2859–2878.

Medina I, Ghose S & Ben-Ari Y (1999). Mobilization of intracellular calcium stores participates in the rise of $[Ca^{2+}]_i$ and the toxic actions of the HIV coat protein GP120. *Eur J Neurosci* **11**, 1167–1178.

Meucci O, Fatatis A, Simen AA, Bushell TJ, Gray PW & Miller RJ (1998). Chemokines regulate hippocampal neuronal signaling and gp120 neurotoxicity. *Proc Natl Acad Sci U S A* **95**, 14500–14505.

Mienville JM (1998). Persistent depolarizing action of GABA in rat Cajal–Retzius cells. *J Physiol* **512**, 809–817.

Mienville JM (1999). Cajal–Retzius cell physiology: just in time to bridge the 20th century. *Cereb Cortex* **9**, 776–782.

Mienville JM & Pesold C (1999). Low resting potential and postnatal upregulation of NMDA receptors may cause Cajal–Retzius cell death. *J Neurosci* **19**, 1636–1646.

Myszka DG, Sweet RW, Hensley P, Brigham-Burke M, Kwong PD, Hendrickson WA *et al*. (2000). Energetics of the HIV gp120-CD4 binding reaction. *Proc Natl Acad Sci U S A* **97**, 9026–9031.

Naumann U, Cameroni E, Pruenster M, Mahabaleshwar H, Raz E, Zerwes HG *et al*. (2010). CXCR7 functions as a scavenger for CXCL12 and CXCL11. *PLoS One* **5**, e9175.

Ogawa M, Miyata T, Nakajima K, Yagyu K, Seike M, Ikenaka K *et al*. (1995). The reeler gene-associated antigen on Cajal–Retzius neurons is a crucial molecule for laminar organization of cortical neurons. *Neuron* **14**, 899–912.

Oh SK, Cruikshank WW, Raina J, Blanchard GC, Adler WH, Walker J & Kornfeld H (1992). Identification of HIV-1 envelope glycoprotein in the serum of AIDS and ARC patients. *J Acquir Immune Defic Syndr* **5**, 251–256.

Oh SB, Tran PB, Gillard SE, Hurley RW, Hammond DL & Miller RJ (2001). Chemokines and glycoprotein120 produce pain hypersensitivity by directly exciting primary nociceptive neurons. *J Neurosci* **21**, 5027–5035.

Omri B, Crisanti P, Alliot F, Marty MC, Rutin J, Levallois C, Privat A & Pessac B (1994). CD4 expression in neurons of the central nervous system. *Int Immunol* **6**, 377–385.

Paredes MF, Li G, Berger O, Baraban SC & Pleasure SJ (2006). Stromal-derived factor-1 (CXCL12) regulates laminar position of Cajal–Retzius cells in normal and dysplastic brains. *J Neurosci* **26**, 9404–9412.

Pozas E, Paco S, Soriano E & Aguado F (2008). Cajal–Retzius cells fail to trigger the developmental expression of the Cl^- extruding co-transporter KCC2. *Brain Res* **1239**, 85–91.

Qian X, Niu X & Magleby KL (2006). Intra- and intersubunit cooperativity in activation of BK channels by Ca^{2+}. *J Gen Physiol* **128**, 389–404.

Radnikow G, Feldmeyer D & Lübke J (2002). Axonal projection, input and output synapses, and synaptic physiology of Cajal–Retzius cells in the developing rat neocortex. *J Neurosci* **22**, 6908–6919.

Rychert J, Strick D, Bazner S, Robinson J & Rosenberg E (2010). Detection of HIV gp120 in plasma during early HIV infection is associated with increased proinflammatory and immunoregulatory cytokines. *AIDS Res Hum Retroviruses* **26**, 1139–1145.

Sattentau QJ & Weiss RA (1998). The CD4 antigen: physiological ligand and HIV receptor. *Cell* **52**, 631–633.

Schönemeier B, Kolodziej A, Schulz S, Jacobs S, Hoellt V & Stumm R (2008). Regional and cellular localization of the CXCl12/SDF-1 chemokine receptor CXCR7 in the developing and adult rat brain. *J Comp Neurol* **510**, 207–220.

Soda T, Nakashima R, Watanabe D, Nakajima K, Pastan I & Nakanishi S (2003). Segregation and coactivation of developing neocortical layer 1 neurons. *J Neurosci* **23**, 6272–6279.

Sodickson DL & Bean BP (1996). GABAB receptor-activated inwardly rectifying potassium current in dissociated hippocampal CA3 neurons. *J Neurosci* **16**, 6374–6385.

Soriano E & Del Río JA (2005). The cells of Cajal–Retzius: still a mystery one century after. *Neuron* **46**, 389–394.

Spitzer NC (2006). Electrical activity in early neuronal development. *Nature* **444**, 707–712.

Stoltenburg G, Schmidt S, Märzheuser S, Herbst H, Spiegel H & Unger M (1991). Das Zentralnervensystem von Kindern HIV-positiver Mütter – Neuropathologie, Immunhistochemie und in-situ-Hybridization. *Verh Dtsch Ges Pathol* **75**, 191–194.

Stumm RK, Rummel J, Junker V, Culmsee C, Pfeiffer M, Krieglstein J *et al*. (2002). A dual role for the SDF-1/CXCR4 chemokine receptor system in adult brain: isoform-selective regulation of SDF-1 expression modulates CXCR4-dependent neuronal plasticity and cerebral leukocyte recruitment after focal ischemia. *J Neurosci* **22**, 5865–5878.

Stumm RK, Zhou C, Ara T, Lazarini F, Dubois-Dalcq M, Nagasawa T *et al*. (2003). CXCR4 regulates interneuron migration in the developing neocortex. *J Neurosci* **23**, 5123–5130.

Supèr H, Martínez A, Del Río JA & Soriano E (1998). Involvement of distinct pioneer neurons in the formation of layer-specific connections in the hippocampus. *J Neurosci* **18**, 4616–4626.

Tinnes S, Schäfer MK, Flubacher A, Münzner G, Frotscher M & Haas CA (2011). Epileptiform activity interferes with proteolytic processing of Reelin required for dentate granule cell positioning. *FASEB J* **25**, 1002–1013.

Tiveron MC, Boutin C, Daou P, Moepps B, Cremer H (2010). Expression and function of CXCR7 in the mouse forebrain. *J Neuroimmunol* **224**, 72–79.

Tran PB, Ren D & Miller RJ (2005). The HIV-1 coat protein gp120 regulates CXCR4-mediated signaling in neural progenitor cells. *J Neuroimmunol* **160**, 68–76.

Womack MD & Khodakhah K (2002). Characterization of large conductance Ca^{2+}-activated K^+ channels in cerebellar Purkinje neurons. *Eur J Neurosci* **16**, 1214–1222.

Xu C, Liu J, Chen L, Liang S, Fujii N, Tamamura H & Xiong H (2011). HIV-1 gp120 enhances outward potassium current via CXCR4 and cAMP-dependent protein kinase a signaling in cultured rat microglia. *Glia* **59**, 997–1007.

Author contributions

Conception and design of the experiments: I.M. and G.M. Collection, analysis and interpretation of the data: all authors. Drafting the article or revising it critically for important intellectual content: all authors. All authors approved the final version.

Acknowledgements

We thank Drs Richard Miller and Marco Martina for comments on a previous version of the manuscript and discussion. This work was supported by the National Institute of Neurological Disorders and Stroke (NINDS) (NS064135, G.M.).

Author's present address

I. Marchionni: 139 Irvine Hall, Department of Anatomy & Neurobiology, University of California, Irvine, CA 92617-1280, USA.